Development and Utilization of Regional Oceanic Modeling System (ROMS).
Delicacy, Imprecision, and Uncertainty of Oceanic Simulations: An Investigation with the Regional Oceanic Modeling System (ROMS).
Submesoscale Flows and Mixing in the Ocean Surface Layer Using the Regional Oceanic Modeling System (ROMS).
Eddy Effects in General Circulation, Spanning Mean Currents, Mesoscale Eddies, and Topographic Generation, including Submesoscale Nests.

James C. McWilliams, M. Jeroen Molemaker, Alexander F. Shchepetkin
Department of Atmospheric and Oceanic Sciences and
University of California, Los Angeles, CA 90095-1565
phone:(310)206-2829 fax:(310)206-5219 email:jcm@atmos.ucla.edu

N00014-08-1-0597, N00014-10-1-0484, N00014-11-1-0726, N00014-12-1-0105, N00014-12-1-0939
http://www.atmos.ucla.edu/roms/

LONG-TERM GOALS

Our long-term goal is the continuing evolution of the Regional Oceanic Modeling System (ROMS) as a multi-scale, multi-process model and its utilization for studying a variety of oceanic phenomena. The dynamical processes span a range from turbulence to basin-scale circulation. A complementary goal is to explore, document, and explain the nature of the delicacies of the simulations for highly turbulent flows.

OBJECTIVES

Our primary objectives are code improvements and oceanographic simulation studies with ROMS, as well as with Large Eddy Simulation (LES) for boundary layer turbulence, with measurement comparisons where feasible. The targeted phenomena are submesoscale wakes, fronts, and eddies; shelf and nearshore currents; internal tides; regional and Pacific eddy-resolving circulations and their low-frequency variability; mesoscale ocean-atmosphere coupling; and planetary boundary layers with surface gravity waves. A parallel objective is to establish the characteristics of model uncertainty in ROMS for realistic simulation of complex flows, as an intrinsic model contribution to analysis and to forecast errors. The premise is that defensible alternative model designs — in parameter values, subgrid-scale parameterizations, resolution, algorithms, topography, and forcing data — may often provide a range of answers comparable to the model-measurement discrepancies. We hypothesize that some part of the model-to-measurement and model-to-model differences may be irreducibly inherent in the mathematical structure of modern simulation models.

APPROACH

To address these problems we are making ROMS more of a multi-process, multi-purpose, multi-scale model by including the coupling of the core circulation dynamics to surface gravity waves; sediment resuspension and transport; biogeochemistry and ecosystems; non-hydrostatic large-eddy simulation; and mesoscale atmospheric circulation, and by providing a framework for data-assimilation analyses

Report Documentation Page

Form Approved
OMB No. 0704-0188

1. REPORT DATE	2. REPORT TYPE	3. DATES COVERED
30 SEP 2012		**00-00-2012 to 00-00-2012**

4. TITLE AND SUBTITLE	5a. CONTRACT NUMBER
Development and Utilization of Regional Oceanic Modeling System (ROMS). Delicacy, Imprecision, and Uncertainty of Oceanic Simulations: An Investigation with the Regional Oceanic Modeling System (ROMS). Submesoscale Flows and Mixing in the Ocean Surface Layer Using the Regional Oceanic Modeling System (ROMS). Eddy Effects in General Circulation, Spanning Mean Currents, Mesoscale Eddies, and Topographic Generation, including Submesoscale Nests.	5b. GRANT NUMBER
	5c. PROGRAM ELEMENT NUMBER
6. AUTHOR(S)	5d. PROJECT NUMBER
	5e. TASK NUMBER
	5f. WORK UNIT NUMBER
7. PERFORMING ORGANIZATION NAME(S) AND ADDRESS(ES) **University of California, Los Angeles,Department of Atmospheric and Oceanic Sciences,Los Angeles,CA,90095-1565**	8. PERFORMING ORGANIZATION REPORT NUMBER
9. SPONSORING/MONITORING AGENCY NAME(S) AND ADDRESS(ES)	10. SPONSOR/MONITOR'S ACRONYM(S)
	11. SPONSOR/MONITOR'S REPORT NUMBER(S)

12. DISTRIBUTION/AVAILABILITY STATEMENT
Approved for public release; distribution unlimited

13. SUPPLEMENTARY NOTES

14. ABSTRACT

15. SUBJECT TERMS

16. SECURITY CLASSIFICATION OF:			17. LIMITATION OF ABSTRACT	18. NUMBER OF PAGES	19a. NAME OF RESPONSIBLE PERSON
a. REPORT **unclassified**	b. ABSTRACT **unclassified**	c. THIS PAGE **unclassified**	**Same as Report (SAR)**	**18**	

(led by others). Our major algorithmic objectives are cross-scale grid-nesting in turbulent flows; accurate advection; dynamically adaptive vertical coordinates; and parameterization of wave-breaking and other mixing effects. Finally, we continue to further improve the pre- and post-processing tools and on-line documentation for ROMS. To test the hypothesis of irreducible uncertainty, we use ROMS to evaluate model sensitivity with respect to plausible variations in several test configurations: flow past idealized sea mounts; realistic Pacific and Atlantic basin circulations comparable to present and near-future operational analysis configurations; and nested regional subdomain currents and eddies with mesoscale and submesoscale flow-topography interaction.

WORK COMPLETED

In the past year we have worked on the following circulation regimes and phenomena: decadal Pacific and Atlantic circulations; equilibrium regional circulations along the U.S. West Coast, central Alaska, Central America, South America, Solomon Sea, the Kuroshio, and the Gulf Stream; mesoscale eddy buoyancy fluxes; submesoscale surface fronts, filaments, and eddies; topographic current separation, form stress, and submesoscale vortex generation; surface waves and nearshore currents and internal tides in Southern California; surface wave influences on the turbulent boundary layer; bubbles generated by wave breaking; and mesoscale air-sea coupling. The algorithmic work has been on adapting the oceanic equation of state for split-explicit time stepping of barotropic and baroclinic modes; accurate time-stepping for the bottom boundary layer in shallow water ($\sim$ meters) and wake flows past topography; open boundary conditions for highly turbulent flows; incorporating surface wave effects in ROMS; diagnosing spurious diapycnal mixing due to advection errors and designing remedies; a new model of a size-distributed bubble population; and the exploration of several test-bed configurations for the simulation delicacy investigation.

RESULTS

We present a few highlights. The publications list (papers from 2011 up to ones likely to be submitted in 2012) provides a view of finalized results.

Basin scale circulation and eddy transports: Widespread experience in basin-scale oceanic modeling indicates a high degree of sensitivity of strong currents to many aspects of the simulation configuration. In Lemarie (2012a) we show a extensive investigation of the sensitivity of the circulation in the Pacific basin to model formulation and forcing. We demonstrate that a modified advection algorithm with implicit diffusion rotated to align with isopycnal surfaces is able to reduce the amount of diapycnal mixing in the ocean interior results in a great improvement in the representation of tracer distribution of water masses at the scales of the large scale circulation. The modified advection scheme, KPP boundary layer mixing, and a new vertical grid are used to implement a ROMS basin-scale 0.5^0 Pacific configuration. Comparisons with various observational datasets are carried out to evaluate the quality of our results in terms of mixed-layer depth, tracer distribution, horizontal circulation, and seasonal variability. ROMS gives results comparable to existing climate models in this way showing its ability to deal with large-scale oceanic flows. Rotating the tracer hyperdiffusion from an iso-sigma to isopycnal direction proves to improve the intermediate water representation (Fig. 1) and the Equatorial Pacific thermocline structure (Fig. 2). An overall tightening of the thermocline is observed, leading to a more realistic Equatorial Undercurrent.

We have repeated this process for the Atlantic basin. Figure 3 shows the successfully simulation

mean path of the Gulf Stream near the eastern seaboard. This high resolution simulation encompasses the full Atlantic basin with its southern boundary near the Antarctic Circumpolar Current and has a mean resolution of $6\ km$. In addition to the Gulf Stream, validation shows many successfully simulation aspects of the Atlantic circulation, some of which are notoriously difficult to model such as the Gibraltar overflow waters and the mid-ocean Azores Current.

Buoyancy and tracer fluxes by mesoscale eddies are an important part of the mean circulation and climate in many places in the ocean. In simulations of Eastern Boundary Systems off North and South America, the eddies provide an offshore cooling and onshore warming to balance the widespread air-sea heating and coastal upwelling cooling, as well as an upward re-stratifying buoyancy flux. This occurs through an eddy-induced Lagrangian mean (bolus) zonal overturning circulation counter to the Eulerian Ekman-upwelling circulation cell, consistent with a parameterization principle as release of the available potential energy of the alongshore current (Colas *et al.*, 2012a,c). In addition, eddy nutrient fluxes along offshore-descending isopycnal surfaces deplete the biological productivity of the upwelling system (Gruber *et al.*, 2011).

Surface submesoscale fronts and filaments: Our focus is on situations where mesoscale energy transfer exchange with submesoscale unbalanced motions is likely to occur. Due to an rapidly expanding set of investigation on oceanic flows at submesoscales, it is increasingly clear that these phenomena are ubiquitous. We are in the process of systematically investigating a range of submesoscale surface phenomena that fall into the broad categories of front, filaments and vortical structures. We illustrate with a few examples.

South of the Gulf Stream separation point at Cape Hatteras, interactions between the North wall of the Gulf stream and undulation of the shelf break lead to a phenomena known as a shingle eddy. Figure 4 shows an evolving shingle eddy near the coast of North Carolina. Diagnostics show that these structures have strong interactions with the shelf break leading to enhance vertical exchanges. Also visible in Fig. 4 is an example of a cold filament (inside the area indicated by the dashed rectangle). This filament, which has strong downward velocities at its core, becomes unstable to instabilities that are fueled by horizontal shear instead.

After separation, the North Wall of the Gulf Stream, exhibits regions with intense, small scale vorticity structures (Fig. 5). These flows are driven by the horizontal, cyclonic shear of the Gulf Stream and again are characterized by large vertical exchange velocities. The reason for asymmetry in the north and south shear regions of the Gulf Stream is the fact that anti-cyclonic shear values are strictly limited by the condition for inertial instability. This limits the anti-cyclonic values to lower values than $-f$ while no such limit exists for the cyclonic shear rates. As recently as the winter of 2012, these structures have been observed within the context of the ONR LATMIX program (private communication, Eric D'Asaro).

In Fig. 6, a model solution of a mesoscale eddy in the Gulf Stream area is shown in normalized surface relative vorticity. The eddy can be seen to be unstable to much smaller scale instabilities around its rim. These modes are hypothesized to be mixed layer instabilities that are essentially geostrophic in nature but have a smaller horizontal scale due to the reduced scale of the Rossby deformation radius in the mixed layer. The small scale rim instability is remarkably persistent throughout the life cycle of the mesoscale eddy. Azimuthal mode decomposition of the structure reveals that low modes that are energized by the environmental straining field act to re-energize the eddy available potential energy field, which allows the rim instability that is driven by release of potential energy to persist. This is an example of the capability of ROMS to compute physically

relevant solutions that can be related to small scale, complex observed phenomena.

Interactions with topography: In recent publications we have shown that subsurface currents may interact with topographic features leading to the formation of coherent anti-cyclonic subsurface mesoscale eddies and locally enhance diapycnal mixing and energy dissipation (Molemaker *et al.*, 2102). More recently, we have focused on the role of interactions with complex topography in the global budget of vorticity. Specifically, the interaction of strong western boundary currents with topography are investigated. Early results point to a much more important contribution from the torque of the bottom pressure in western boundary regions than previously thought. Figure 7 shows the contribution for the torque of bottom pressure on the barotropic vorticity equation in the Gulf Stream path. For illustration purposes, the bottom torque is only shown in the core of the Gulf Stream. While not uniform in sign, the integration of this signal along the path of the Gulf Stream shows a positive contribution of barotropic vorticity that is an order of magnitude larger than the contribution of frictional processes. We intend to replicate this diagnostic in several other areas around the globe for which we have numerical solutions such as the Solomon Sea and the Kuroshio region near Japan.

Surface wave effects in the boundary layer: Surface waves influence boundary layer currents through vortex force and tracer advection by Stokes drift and through breakers that inject momentum, energy, and bubbles. In simulations of the canonical Ekman problem (steady wind, equilibrium waves, no stratification), we find that waves deepen the layer by enhanced momentum transport associated with Langmuir circulations, and the most apt representation is as a mixing of the Lagrangian mean current (McWilliams *et al.*, 2012). In the transient wind and wave evolution under a hurricane, wave-induced variations in the thermocline entrainment rate enhance surface temperature differences between the left and right sides of the storm in combination with the effects of inertial-wave resonance (Sullivan *et al.*, 2012). Current research is on how remotely generated swell waves combine with local wind waves to modify the mean Ekman current. Bubble clouds are carried into the boundary layer in the downwelling branches of Langmuir circulations; their penetration depth increases with wind speed, and the model simulations match observations fairly well (Fig. 8). As a consequence of increasing pressure with depth, the gas dissolution from the bubbles leads to supersaturation even in air-sea equilibrium. Using LES simulations at different wind speeds we developed a new parameterization of air-sea gas exchange and find that this supersaturation effect causes a measurable difference even in abyssal gas concentration (Liang *et al.*, 2012c).

Sensitivity of oceanic simulations to forcing, topography, and algorithms: As discussed above for the Gulf Stream, we find great sensitivity of the path of the Kuroshio to changes in topography and land boundaries, both local and remote such as changes to the land mask in the Solomon sea. Additionally, exploration of the influences of the wind forcing had already shown great sensitivity of equatorial current structure to wind forcing (Lemarie *et al.* , 2012a). Current research shows additional sensitivity of the path of the Gulf Stream to small changes in remote wind forcing patterns. Modifying the way that wind forcing is extended toward land boundaries has led to changes in the forcing primarily in the far Northern Atlantic due to missing observational data over sea ice. These remote changes lead to changes in the mean path of the Gulf Stream in the Cape Hatteras area. In general, it is clear that there are uncertainties in the ingredients of an ocean circulation model, such as the different surface forcing field, that, while small, lead to significant changes in the resulting circulation. Finally, the Pacific circulation simulations in Lemarie *et al.* (2012a) contain demonstrations of algorithmic sensitivities for the advection, KPP parameterization, and vertical grid (*e.g.,* , Figs. 1-2). We are reporting on these forcing, topographic, and algorithmic sensitivities within

the context of the dynamical subjects of our papers.

Improving efficiency of MPI routines and computing practices: Recently we have implemented several measures to improve code performance, robustness, and reproducibility, and to adapt to the evolving computing environment. outstanding for a long time issue of the running ROMS as a multi-threaded (Open MP) code multi-core node vs. the performance of code using MPI the same problem using the same hardware (i.e., MPI running only a single node): the multi-threaded code with optimal subdomain partitioning significantly outperforms MPI, however this obviously cannot vertically integrated momentum equations separately using a much smaller time step, it exchanges messages of two significantly different sizes: a larger one associated with halo-exchange for 3D arrays, and a smaller one for 2D. It is well known that MPI transmission bandwidth strongly depends on message size in a rather complex way, Fig. 9. Small messages are severely penalized by start-up latencies, while the decline for very large messages is more complicated to explain, but it is also less important for our purposes because message sizes exceeding $10,000$ would occur only for a hypothetically large subdomain size of 100^3, at which point (actually even before that, as follows from the past experience with UCLA ROMS) it is advantageous to introduce inner partitioning within each MPI subdomain (this is motivated by cache optimization), which will also split such very large messages. On the other hand, for most of our configurations the size of halo-exchange messages for 2D arrays is within the low hundreds, placing them to the lower-left corner on Fig. 9, far below the size where a significant fraction of theoretical bandwidth can be achieved. To counter this we have combined messages exchanging ghost points of different arrays into larger messages exchanging more than one array (up to 4) in a single message passing session whenever it is possible. This requires logical rearrangement of the code; however, this is fortunately coincident with the structural requirements associated with maintaining both MPI and Open MP parallelizations within the same code (*e.g.,* all message passing must occur only at the very end before Open MP synchronization events (and is prohibited elsewhere), and the desirability of reducing the number of synchronizations for efficiency, achieved by admitting a small amount of redundant computations near the subdomain edges in order to delay synchronization events). After this revision the situations where halos for a single 2D array are exchanged in separate session are excluded completely; 2D arrays exchanged within the 3D part of the code are "attached" to the 3D messages, and the barotropic mode prognostic variables ζ, $\overline{u}$, $\overline{v}$ are exchanged in a single session. In practice we find an overall performance gain of $\sim 40\%$ for a $1600\times560\times32$ grid running on 32 nodes (256 CPU cores total) relative to the same code except for exchanging arrays individually.

IMPACT/APPLICATIONS

Geochemistry and Ecosystems: An important community use for ROMS is biogeochemisty: chemical cycles, water quality, blooms, micro-nutrients, larval dispersal, biome transitions, and coupling to higher tropic levels. We collaborate with Profs. Keith Stolzenbach (UCLA), Niki Gruber (ETH), Curtis Deutsch (UCLA), David Siegel (UCSB), and Yusuke Uchiyama (Kobe).

Data Assimilation: We collaborate with Drs. Zhinjin Li (JPL), Yi Chao (Remote Sensing Solutions), and Kayo Ide (U. Maryland) by developing model configurations for targeted regions and by consulting on the data-assimilation system design and performance. Current quasi-operational, 3DVar applications are in California (SCCOOS and CenCOOS) and in Alaska (Prince William Sound).

TRANSITIONS

ROMS is a community code with widespread applications (http://www.myroms.org).

RELATED PROJECTS

Three Integrated Ocean Observing System (IOOS) regional projects for California and Alaska (SCCOOS, CenCOOS, and AOOS) are utilizing ROMS for data assimilation analyses and forecasts.

PUBLICATIONS

Baschek, B., M. Abramcyzyk, D. Stokes, G. Deane, J.H. Liang, & J.C. McWilliams, 2012: Direct laboratory seawater measurements of the dissolved CO2 signature of individual breaking waves. *J. Geophys. Res.*, submitted.

Boe, J., A. Hall, F. Colas, J. McWilliams, X. Qu, & J. Kurian, 2011: What shapes mesoscale wind anomalies in coastal upwelling zones? *Climate Dynamics* **36**, 871-877.

Buijsman, M.C., Y. Uchiyama, J.C. McWilliams, & C.R. Hill-Lindsay, 2011: Modeling semidiurnal internal tide variability in the Southern California Bight. *J. Phys. Ocean.* **42**, 62-77.

Colas, F., J.C. McWilliams, X. Capet, & J. Kurian, 2012a: Heat balance and eddies in the Peru-Chile Current System. *Climate Dynamics* **39**, 509-529.

Colas, F., X. Wang, X. Capet, Y. Chao, & J.C. McWilliams, 2012b: Untangling the roles of wind, run-off and tides in Prince William Sound. *Continental Shelf Research*, in press.

Colas, F., X. Capet, X., J.C. McWilliams, and Z. Li, 2012c: Mesoscale eddy buoyancy flux and eddy-induced circulation in eastern-boundary upwelling systems. *J. Phys. Ocean.*, submitted.

Colas, F., X. Capet, X., & J. McWilliams, 2012d: Seasonal and geographical variability of surface-layer submesoscale circulations, in preparation.

Dong, C., J.C. McWilliams, A. Hall, & M. Hughes, 2011a: Numerical simulation of a synoptic event in the Southern California Bight. *J. Geophys. Res.* **116**, C05018.

Dong, C., F. Nencioli, Y. Liu, & J.C. McWilliams, 2011b: An automated approach to detect oceanic eddies from satellite remote sensed Seas Surface Temperature data. *IEEE Geoscience and Remote Sensing Letters* **8**, 1055-1059.

Dong, C., X. Lin,, Y. Liu, F. Nencioli, Y. Chao, Y. Guan, T. Dickey, & J.C. McWilliams, 2012a: Three-dimensional oceanic eddy analysis in the Southern California Bight from a numerical product. *J. Geophys. Res.* **117**, C00H14.

Dong, C., Y. Liu, R. Lumpkin, M. Lankhorst, D. Chen, J.C. McWilliams, & Y. Guan, 2012b: A scheme to identify loops from trajectories of oceanic surface drifters: An application in the Kuroshio Extension region. *J. Atmos. Ocean Tech.*, in press.

Dong, C., J.C. McWilliams, Y. Liu, & D. Chen, 2012c: Global heat and salt transports by eddy movement. *Nature Geosci.*, submitted.

Farrara, J., Y. Chao, Z. Li, X. Wang, X. Jin, H. Zhang, P. Li, Q. Vu, P. Olsson, C. Schoch, M. Halverson, M. Moline. J. McWilliams, & F. Colas, 2012: A data-assimilative ocean forecasting system and an evaluation of its performance during Sound Predictions 2009. *Continental Shelf Research*, submitted.

Gruber, N., Z. Lachkar, H. Frenzel, P. Marchesiello, M. Munnich, J.C. McWilliams, T. Nagai, & G.-K. Plattner, 2011: Eddy-induced reduction of biological production in eastern boundary upwelling systems. *Nature Geophys.* **4**, 787-792.

Kurian, J., F. Colas, X. Capet, J.C. McWilliams, & D.B. Chelton, 2011: Eddy properties in the California Current System,. *J. Geophys. Res.* **116**, C08027, doi:10.1029/2010JC006895.

Lemarie , F., J. Kurian, A.F. Shchepetkin, M.J. Molemaker, F. Colas, & J.C. McWilliams, 2012a: Are there inescapable issues prohibiting the use of terrain-following coordinates in climate models?

Ocean Modelling **42**, 57-79.

Lemarie, F., L. Debreu, L., A.F. Shchepetkin, & J.C. McWilliams, 2012b: On the stability and accuracy of the harmonic and biharmonic adiabatic mixing operators in ocean models. *Ocean Modelling* **52-53**, 9-35.

Li, Z., Y. Chao, J. Farrara, & J.C. McWilliams, 2012a: Impacts of distinct observations during the 2009 Prince William Sound field experiment: A data assimilation study. *Continental Shelf Research*, in press.

Li, Z., Y. Chao, J. McWilliams, K. Ide, & J.D. Farrara, 2012b: A multi-scale three-dimensional variational data assimilation and its application to coastal oceans. *Q. J. Roy. Met. Soc.*, submitted.

Li, Z., Y. Chao, J.C. McWilliams, K. Ide, & J. Farrara, 2012c: Experiments with a multi-scale data assimilation scheme. *Tellus Series A: Dynamic Meteorology and Oceanography*, submitted.

Liang, J.H., J.C. McWilliams, P.P. Sullivan, & B. Baschek, 2011: Modeling bubbles and dissolved gases in the ocean. *J. Geophys. Res.* **116**, C03015.

Liang, J.H., J.C. McWilliams, P.P. Sullivan, & B. Baschek, 2012a: Large Eddy Simulation of the bubbly ocean: Impacts of wave forcing and bubble buoyancy. *J. Geophys. Res.* **117**, C04002.

Liang J.-H., J. C. McWilliams, J. Kurian, P. Wang & F. Colas, 2012b: Mesoscale variability in the Northeastern Tropical Pacific: Forcing mechanisms and eddy properties. *J. Geophys. Res.* **117**, C07003.

Liang, J.-H., C. Deutsch, J. McWillams, B. Baschek, & P. Sullivan, 2012c: Parameterizing surface bubble-induced supersaturation and its impact on the ocean interior. *Glob. Biogeo. Cycles*, submitted.

Liu, Y., C. Dong, Y. Guan, D. Chen, & J.C. McWilliams, 2012: Eddy analysis for the subtropical zonal band of the North Pacific Ocean. *Deep-Sea Res. I* **68**, 54-67.

Mason, E., F. Colas, M. J. Molemaker, A. F. Shchepetkin, C. Troupin, J. C. McWilliams, and P. Sangrà, 2011: Seasonal variability in the Canary Basin: a numerical study. *J. Geophys. Res.* **116**, C06001.

McWilliams, J.C., & M.J. Molemaker, 2011: Baroclinic frontal arrest: A sequel to unstable frontogenesis. *J. Phys. Ocean.* **41**, 601-619.

McWilliams, J.C., E. Huckle, J. Liang, & P. Sullivan, 2012: The wavy Ekman layer: Langmuir circulations, breakers, and Reynolds stress. *J. Phys. Ocean.*, in press.

McWilliams, J.C., & B. Fox-Kemper, 2012: Wave-balanced surface fronts and filaments. *J. Phys. Ocean.*, in preparation.

Menesguen, C., J.C. McWilliams, & M.J. Molemaker, 2012: An example of ageostrophic instability in a rotating stratified flow. *J. Fluid Mech.*, in press.

Molemaker, M.J., & J.C. McWilliams, 2012: The bifurcation structure of decadal thermohaline oscillations. *Geophys. & Astrophys. Fluid Dyn.* **106**, 1-21.

Molemaker, M.J., J.C. McWilliams, & W.K. Dewar, 2012: Submesoscale generation of mesoscale anticyclones in the California Undercurrent. *J. Phys. Ocean.*, submitted.

Restrepo, J.M., J.M. Ramírez, J.C. McWilliams, and M. Banner, 2011: Multi-scale momentum flux and diffusion due to whitecapping in wave/current interactions. *J. Phys. Ocean* **41**, 837-856.

Romero, L.E., Y. Uchiyama, J. McWilliams, C. Ohlmann, and D. Siegel, 2012: Particle-pair dispersion in the Southern California coastal zone. In preparation.

Roullet, G., J.C. McWilliams, X. Capet, & M.J. Molemaker, 2012: Properties of equilibrium geostrophic turbulence with isopycnal outcropping. *J. Phys. Ocean.* **42**, 18-38.

Shchepetkin, A.F., & J.C. McWilliams, 2011: Accurate Boussinesq modeling with a practical, "stiffened" equation of state. *Ocean Modelling* **38**, 41-70.

Sullivan, P.P., L. Romero, J.C. McWilliams, & W.K. Melville, 2012: Transient evolution of Langmuir Turbulence in ocean boundary layers driven by hurricane winds and waves. *J. Phys. Ocean.*, in press.

Uchiyama, Y., E. Idica, J.C. McWilliams, and K. Stolzenbach, 2012: Wastewater effluent dispersal in two Southern California Bays. *Cont. Shelf Res.*, in preparation.

Wang, P., J.C. McWilliams, & Z. Kizner, 2012: Ageostrophic instability in rotating shallow water. *J. Fluid Mech.*, in press.

Wang, X., Y. Chao, H. Zhang, J. Farrara, Z. Li, X. Jin, K. Park, F. Colas, J.C. McWilliams, C. Paternostro. C.K. Shum, Y. Yi, C. Schoch, & P. Olsson, 2012: Modeling tides and their influence on the circulation in Prince William Sound, Alaska. *Continental Shelf Research*, in press.

Watson, J. R., C. G. Hays, P. T. Raimondi, S. Mitarai, D. A. Siegel, C. Dong, J. C. McWilliams, & C. A. Blanchette, 2011: Currents connecting communities: the decay of nearshore community similarity with ocean circulation. *Ecology* **92**, 1193-1200.

Weir, B., Y. Uchiyama, E. M. Lane, J. M. Restrepo, & J. C. McWilliams, 2011: A vortex force analysis of the interaction of rip currents and gravity waves. *J. Geophys. Res.* **116**, C05001.

FIGURES

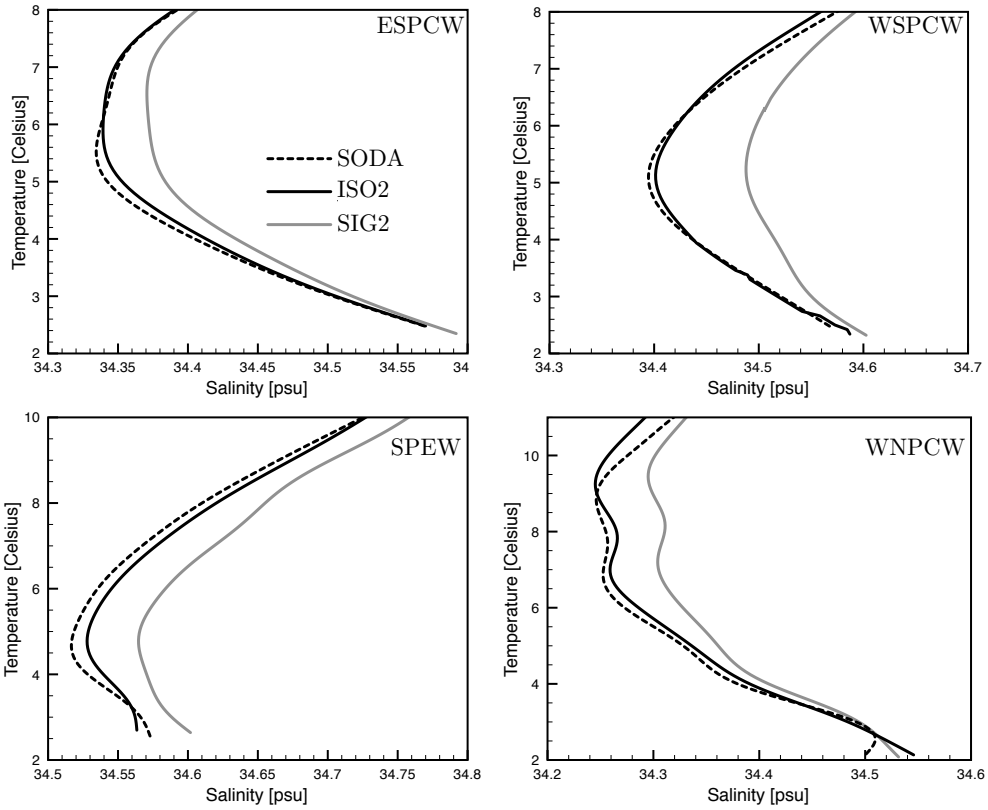

Figure 1: ***Temperature-salinity relationships for four distinct water masses: ESPCW (Eastern South Pacific Central Water, top,left), WSPCW (Western South Pacific Central Water, top,right), SPEW (South and North Pacific Equatorial Water, bottom, left), and WNPCW (Western North Pacific Central Water, bottom, right). The black dotted line corresponds to the SODA climatology used to initialize and force the Pacific model at the boundaries. The ISO*** *(i.e.,* ***with a neutral biharmonic diffusion operator) and SIG*** *(i.e.,* ***with a biharmonic along sigma surfaces) solutions are represented, respectively, by a black and a gray line. False diapycnal fluxes are much reduced in ISO.***

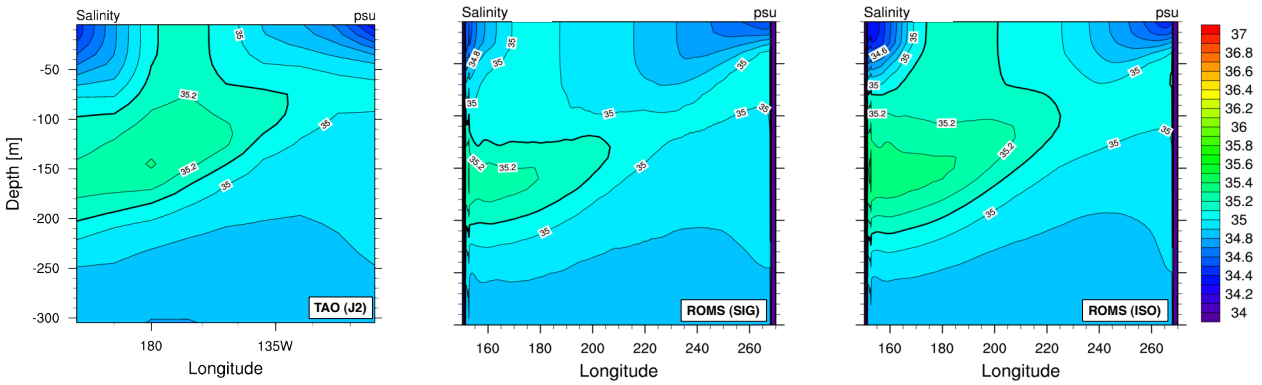

Figure 2: ***Annual climatology of equatorial*** (2^0***S -*** 2^0***N averaged) salinity [PSU] from Johnson et al. (2002) (TAU J2, left), and ROMS SIG (i.e. with biharmonic diffusion along sigma surfaces, middle) and ISO (i.e. with a neutral biharmonic, right) solutions. Again, ISO is more accurate.***

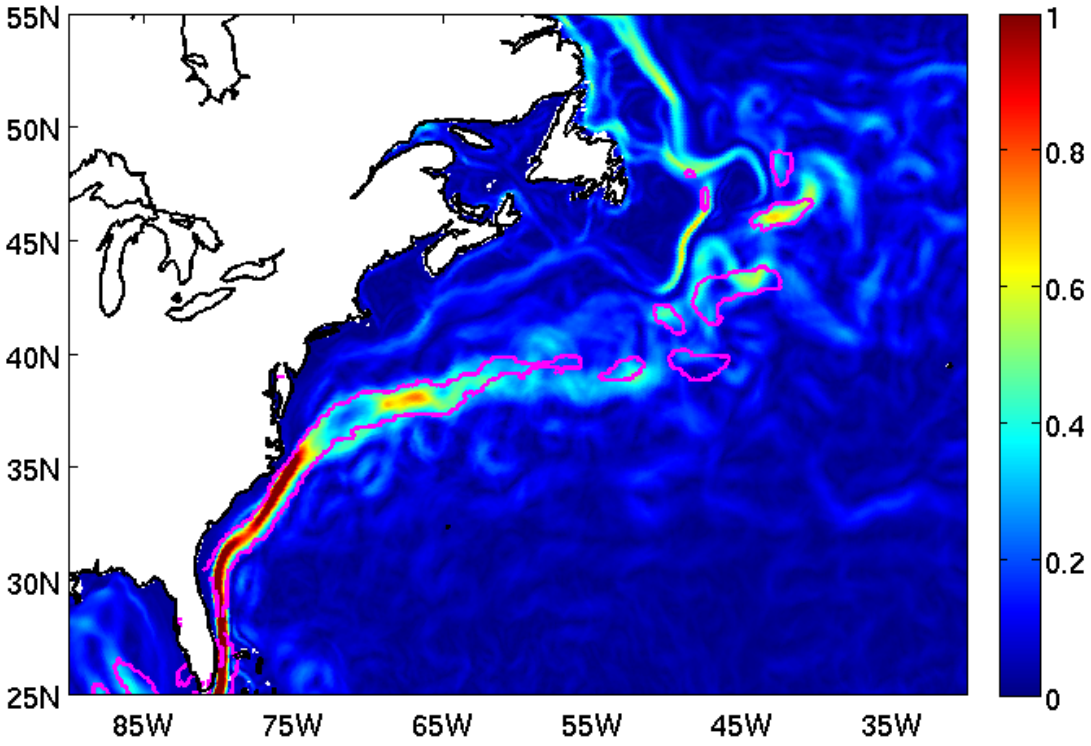

Figure 3: ***Annual mean surface current speed in the Northwest Atlantic showing the mean path of the Gulf Stream. The magenta line shows the 0.3 m/s contour level of surface geostrophic velocities derived from the AVISO altimetry data set.***

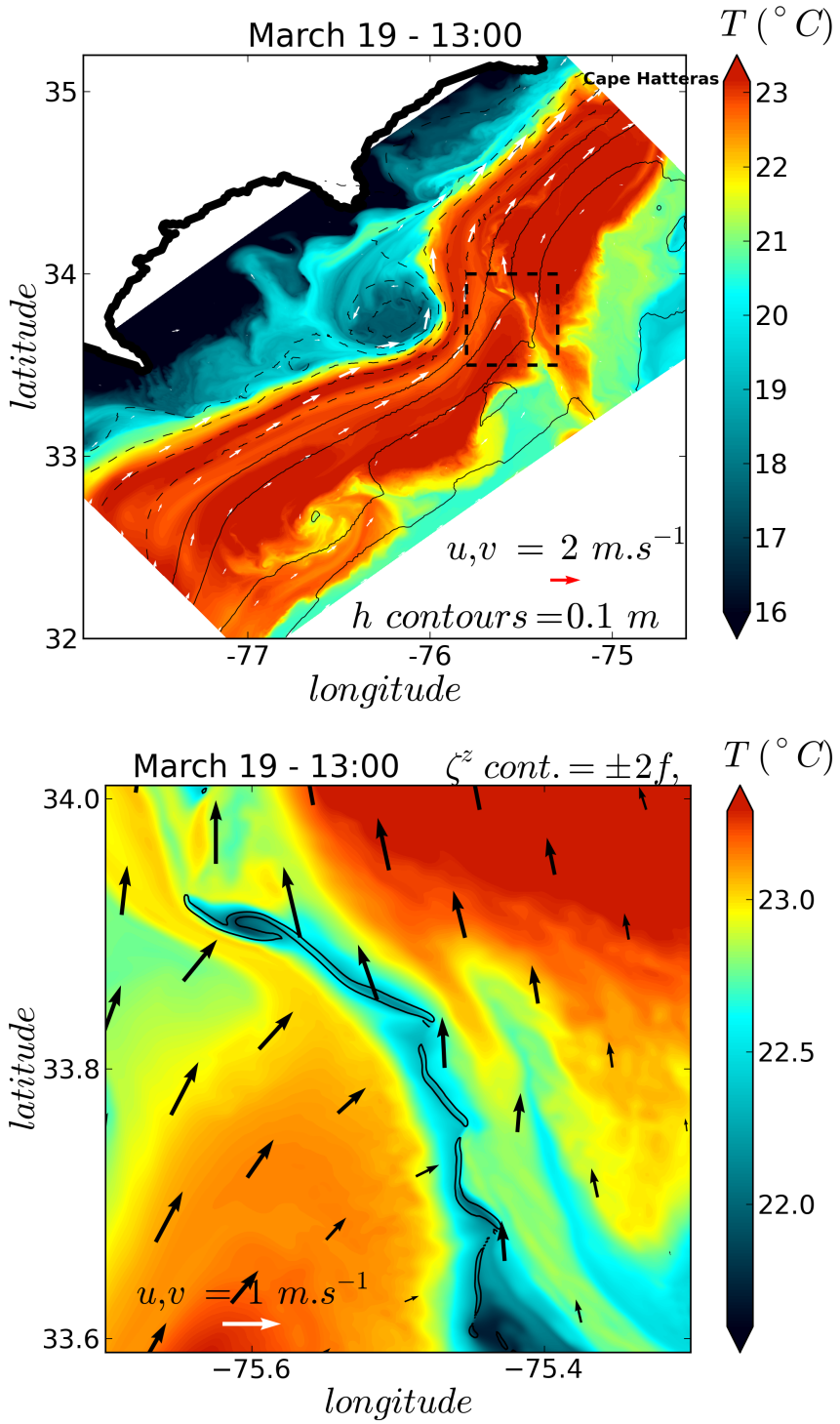

Figure 4: ***Simulated Sea Surface Temperature (SST) for a region south of the Gulf Stream separation point at Cape Hatteras. Surface velocities are the white vectors. The sea surface dynamic height is shown with thin black contour lines. A mesoscale "shingle" eddy is present on the shoreward side of the Gulf Stream, its birth triggered by irregularities on the shelf break. The dashed black rectangle shows a submesoscale cold filament intrusion with strong downward velocities at its center, and the lower panel is a zoom. This filament will break up in the next few days as a result of horizontal shear instabilities.***

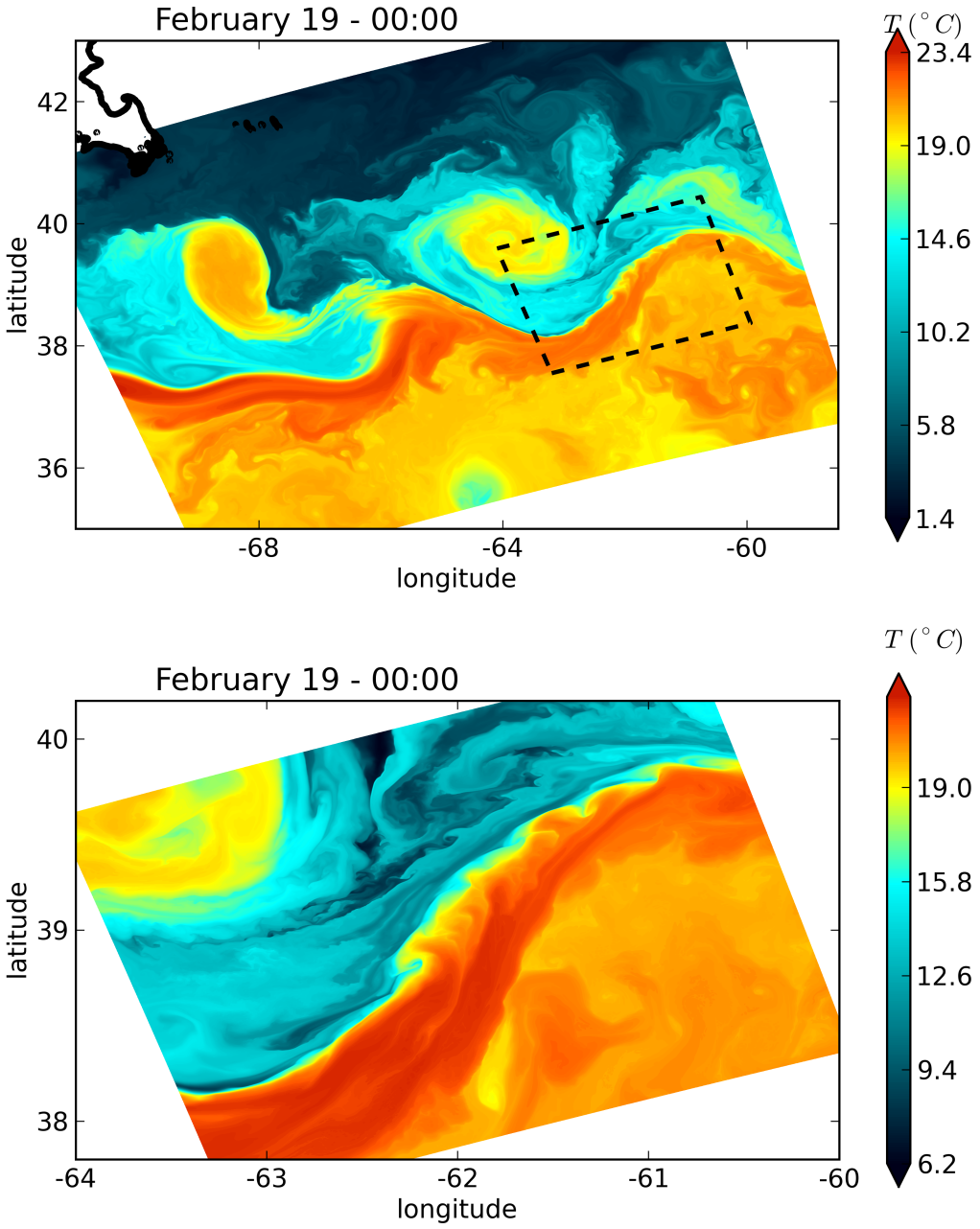

Figure 5: ***Simulated Sea Surface Temperature (SST) for a region downstream of the Gulf Stream separation point at Cape Hatteras. This figures shows a range of submesoscale flow that exist in the presence of mesoscale structures such as the warm-core Gulf Stream Rings to the north and backward streamers off of meander crests. We focus on the submesoscale instability within the rectangular region, with a zoom in the lower panel. The source of energy for this instability the horizontal shear in the North Wall of the Gulf Stream. It has enhanced vertical exchanges and leads to relatively strong local energy dissipation.***

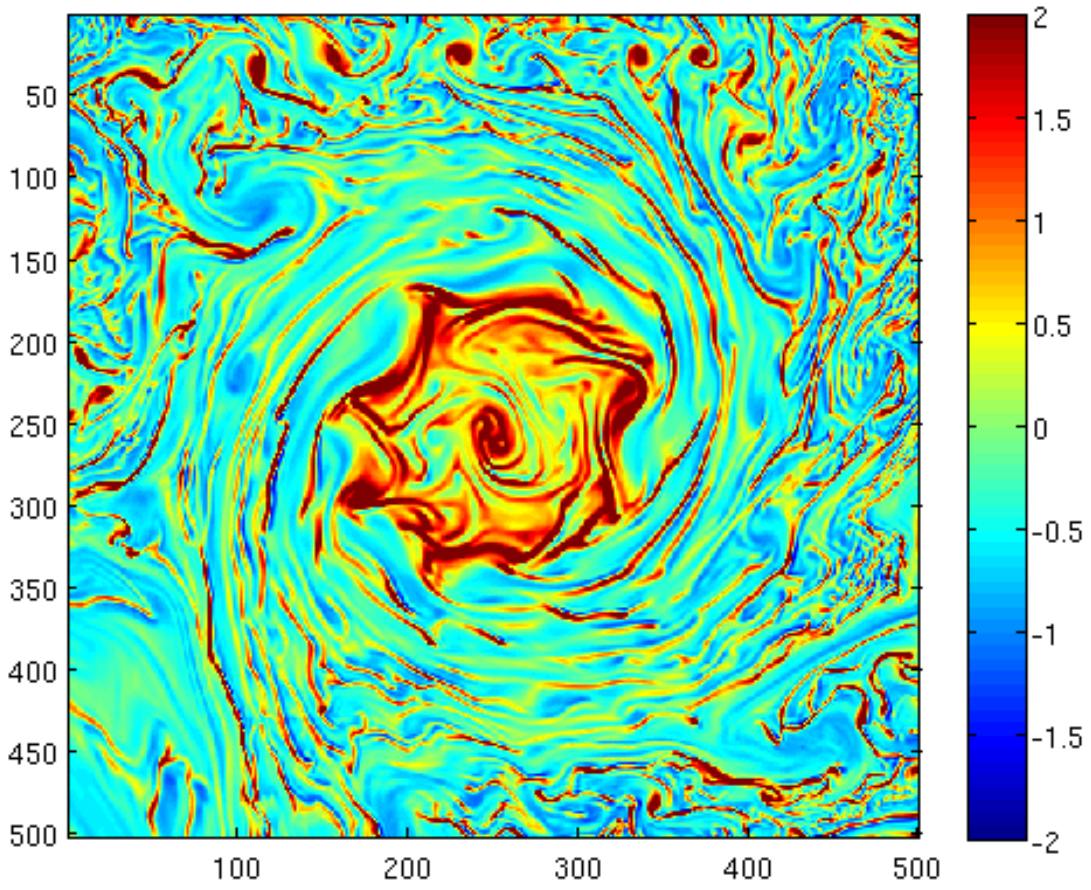

Figure 6: ***Surface relative vorticity showing an anti-cyclonic cold-core Gulf Stream Ring in an area southeast of Cape Hatteras. Clearly visible in the image is the complex submesoscale structure of vorticity inside the ring, which arises from the potential energy contained in the radial density gradients of the Ring. These density gradients are replenished by the low azimuthal modes of oscillations within the Ring, which, in turn, are energized by an interaction of the the ambient straining field with the Ring.***

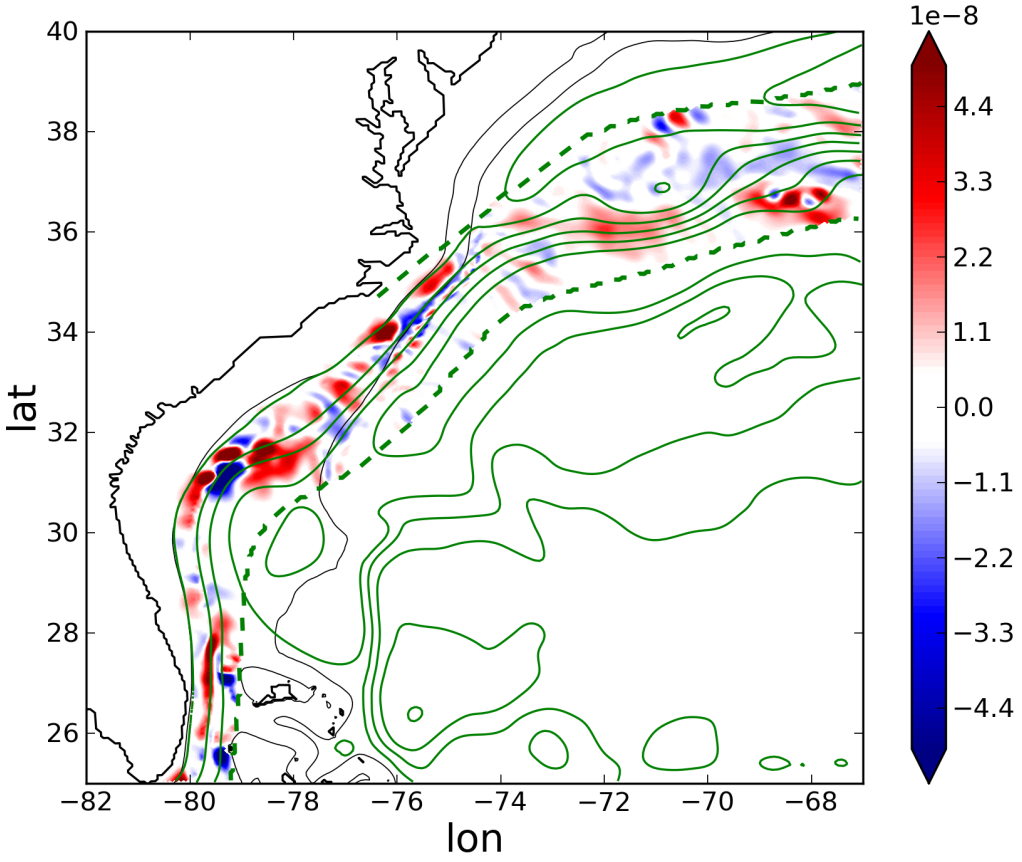

Figure 7: ***Time-mean of bottom pressure torque [m/s^2] within the core of the Gulf Stream (green dashed lines) defined by the peripheral maximum and minimum of barotropiic transport (green contours every 10 Sv). While of both signs near particular topographic features, the torque is pervasively positive (cyclonic) along the Stream, in opposition to the anticyclonic wind curl in the subtropical gyre.***

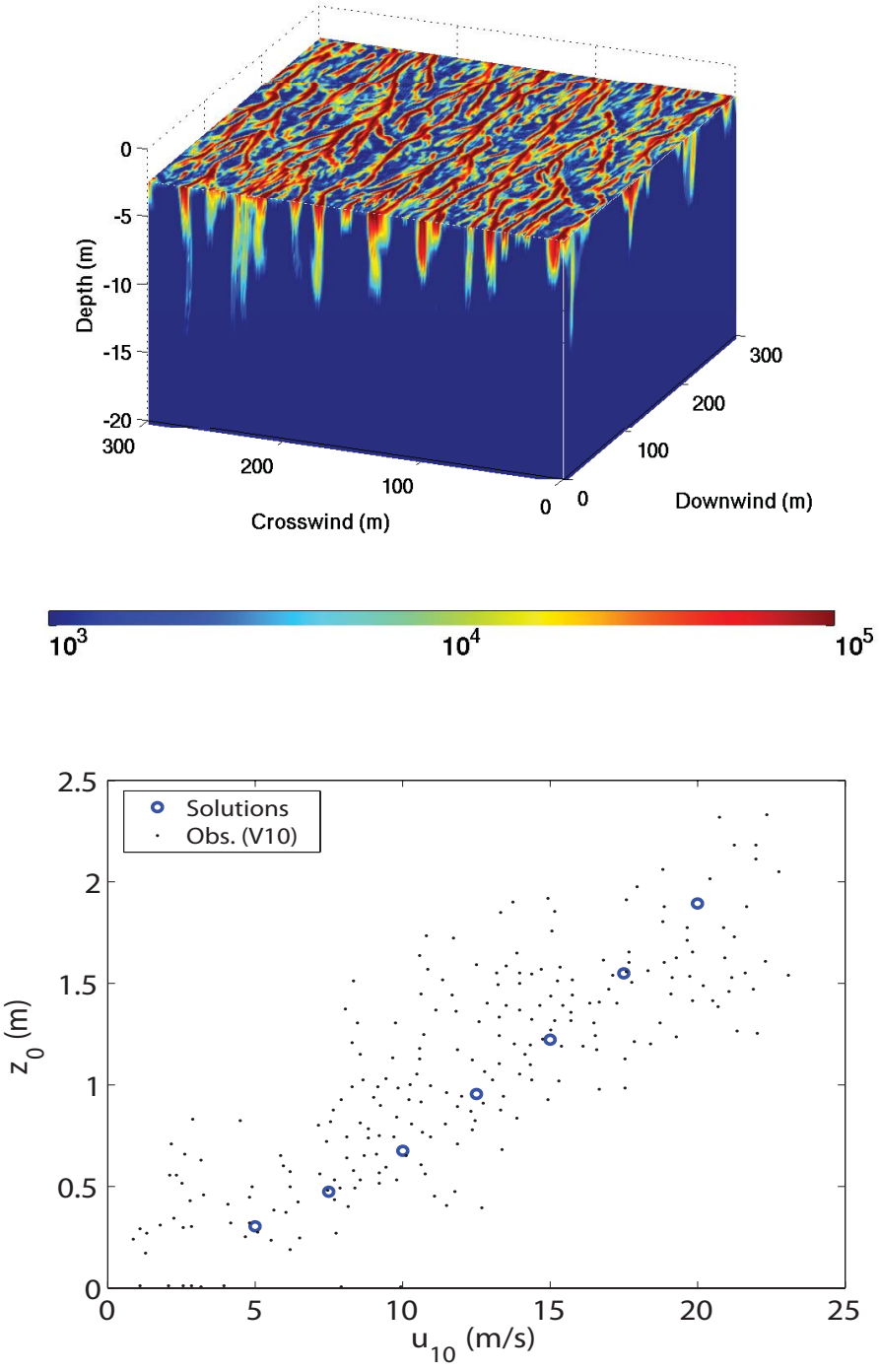

Figure 8: ***Upper panel: An instantaneous snapshot of simulated total bubble number density (number per m^3) in the upper ocean at u10 = 17.5 m/s. Lower panel: Relationship between bubble e-folding depth z0 and wind speed u10. (Black dots: observations by Vagle*** *et al. [J.G.R.,* ***2010]; Blue circles: bubbly flow solutions assuming waves in equilibrium with local winds.) (Liang*** *et al.,* ***2012c)***

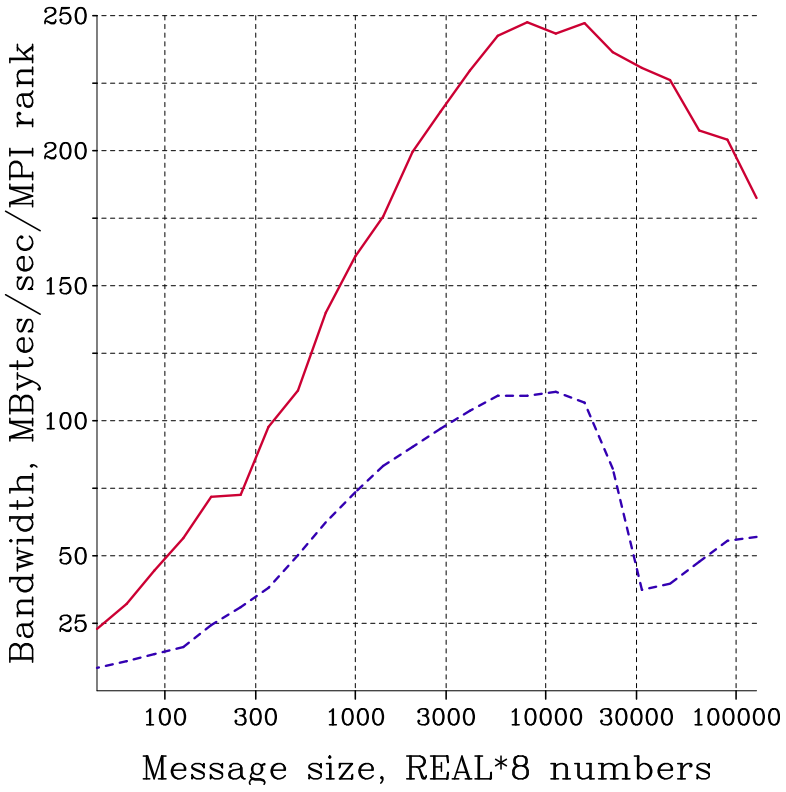

Figure 9: ***Averaged transmission bandwidth as a function of message size.*** **Solid red curve*****: using a cluster made of 8 CPU-core nodes with DDR Infiniband interconnect between them;*** **dashed blue*****: 2 CPUs per node, Gigabit network. The timings were obtained on two different clusters by running a test program which sends and receives messages of a fixed size in a pattern similar to the actual ROMS halo-exchange routines. The bandwidth is measured by tracking the accumulated size of all messages sent by a single MPI process and dividing by the total wall-clock time (hence it is bandwidth per MPI node). As in the actual ROMS code, each MPI process receives exactly the same amount of data as it sends during this test, and the bandwidth reported here is only for sends (or receives) taken separately. The test involves messages sent-received within each multi-CPU node in addition to the messages traveling across the interconnecting fabric. Similarly to the practical usage of ROMS, we explicitly control MPI node mapping onto hardware nodes to maximize the amount of data sent locally within each hardware node and minimize messaging across the network. It should be noted that although Infiniband appears on this plot to be only twice or slightly more better than Gigabit, it should be kept in mind that there are 8 processes on each node competing for the access to the interface vs. 2 processes in the case of Gigabit. The actual difference in bandwidth aggregate per network interface is more dramatic.***